Ziegler, M., Heidbach, O., Zang, A., Martinez Garzon, P., Bohnhoff, M. (2017): Estimation of the differential stress from the stress rotation angle in low permeable rock. - *Geophysical Research Letters*, *44*, pp. 6761—6770.

DOI: http://doi.org/10.1002/2017GL073598

AGU PUBLICATIONS

Geophysical Research Letters

RESEARCH LETTER
10.1002/2017GL073598

Key Points:
- Injection-induced stress tensor rotations can be used to estimate the differential stress
- Controlling factors for stress rotation are permeability, initial differential stress, and injection rate
- Thermal effects have no significant influence on stress rotations

Correspondence to:
M. O. Ziegler,
mziegler@gfz-potsdam.de

Citation:
Ziegler, M. O., O. Heidbach, A. Zang, P. Martínez-Garzón, and M. Bohnhoff (2017), Estimation of the differential stress from the stress rotation angle in low permeable rock, *Geophys. Res. Lett.*, *44*, 6761–6770, doi:10.1002/2017GL073598.

Received 28 MAR 2017
Accepted 4 MAY 2017
Accepted article online 8 MAY 2017
Published online 15 JUL 2017

Estimation of the differential stress from the stress rotation angle in low permeable rock

Moritz O. Ziegler[1,2], Oliver Heidbach[1], Arno Zang[1,2], Patricia Martínez-Garzón[1], and Marco Bohnhoff[1,3]

[1]Helmholtz Centre Potsdam GFZ German Research Centre for Geosciences, Potsdam, Germany, [2]Institute of Earth and Environmental Science, University of Potsdam, Potsdam, Germany, [3]Department of Earth Sciences, Free University Berlin, Berlin, Germany

Abstract Rotations of the principal stress axes are observed as a result of fluid injection into reservoirs. We use a generic, fully coupled 3-D thermo-hydro-mechanical model to investigate systematically the dependence of this stress rotation on different reservoir properties and injection scenarios. We find that permeability, injection rate, and initial differential stress are the key factors, while other reservoir properties only play a negligible role. In particular, we find that thermal effects do not significantly contribute to stress rotations. For reservoir types with usual differential stress and reservoir treatment the occurrence of significant stress rotations is limited to reservoirs with a permeability of less than approximately 10^{-12} m^2. Higher permeability effectively prevents stress rotations to occur. Thus, according to these general findings, the observed principal stress axes rotation can be used as a proxy of the initial differential stress provided that rock permeability and fluid injection rate are known a priori.

Plain Language Summary Rotations of the Earth's stress field are observed due to injections of fluid into (geothermal) reservoirs. We use numerical modeling in order to derive the key parameters that control the amount of stress rotation. We find that the stress rotation is controlled mainly by the permeability of the rock, the rate of fluid injection, and the initial stress field in the reservoir. Since the injection rate is known and the permeability of the reservoir is often estimated, it is possible to gain information on the stress field from observed stress rotations.

1. Introduction

Sustainable and safe subsurface engineering and seismic hazard assessment requires detailed information on the initial stress state [*Cornet et al.*, 1997; *Harris*, 1998; *Zoback*, 2010; *Fuchs and Müller*, 2001; *Heidbach and Ben-Avraham*, 2007]. However, widely available are only the orientation of the maximum horizontal stress S_{Hmax} [*Heidbach et al.*, 2010, 2016; *Zoback*, 2010], while information on the stress magnitudes is very sparse [*Zang et al.*, 2012]. To date, the estimation of the stress magnitudes is only partly possible or economically feasible and remains a challenge [*Brown and Hoek*, 1978; *Brudy et al.*, 1997; *Lund and Zoback*, 1999; *Zang and Stephansson*, 2010].

Though the general knowledge on induced and natural subsurface processes steadily grows due to the often extensive monitoring during the exploitation of geological reservoirs, unconventional hydrocarbons among them, the recordings from local seismic networks operating with a low-magnitude detection threshold and good azimuthal coverage can be used to determine focal mechanism solutions and to apply a stress inversion technique [*Schoenball et al.*, 2014; *Dorbath et al.*, 2009; *Gritto and Jarpe*, 2014]. If a sufficiently high number of seismic events with focal mechanisms is available in a spatially confined area over a certain time period, advanced stress inversion techniques even allow for determining temporal variations of the stress state [*Hardebeck and Michael*, 2006; *Martínez-Garzón et al.*, 2014a] or the 3-D spatial distribution [*Martínez-Garzón et al.*, 2016]. Thereby, temporal local rotations of the stress tensor have been observed as a physical response of the rock formation to large tectonic earthquakes [*Hardebeck and Hauksson*, 2001; *Bohnhoff et al.*, 2006; *Ickrath et al.*, 2015]. Typically, these coseismically introduced stress rotations decrease within weeks or months back to pre–main shock orientations to a large extent [*Hardebeck*, 2012]. More recently, systematic temporal stress

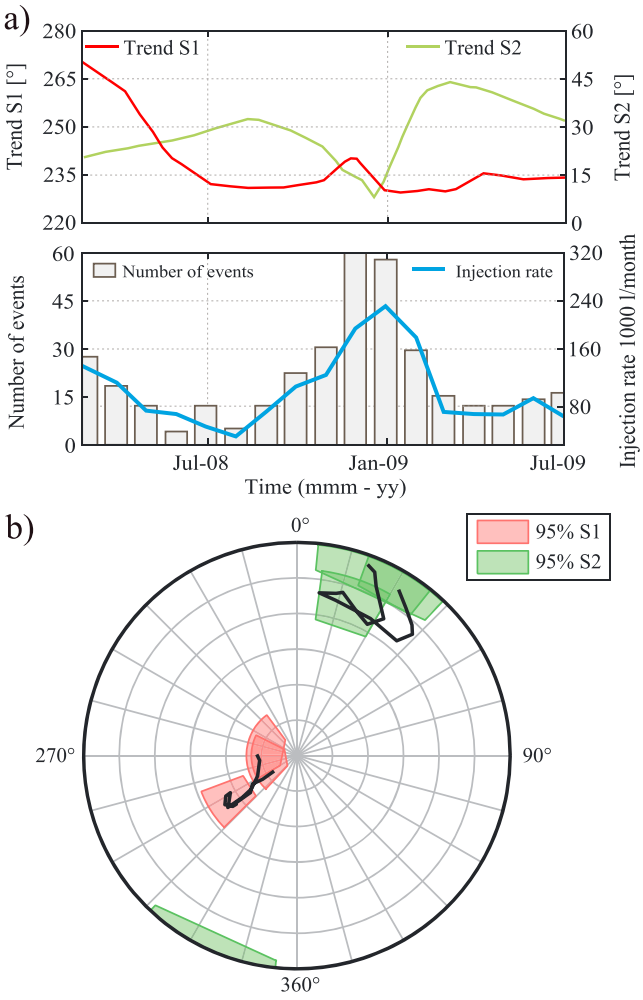

Figure 1. Temporal changes in fluid injection-induced stress rotations in The Geysers NW site, California [*Martínez-Garzón et al.*, 2013]. (a) Rotations in the trend of *S*1 (red) and *S*2 (green) due to fluid injection rate (blue) and number of detected seismic events (grey bars) over the course of 18 months. (b) Schmidt plot of the temporal variations of the initially principal stress axes S1 (red) and S2 (green) during the fluid injection indicated by stress inversions of focal mechanisms. The stress paths (black line) and the 95% confidence intervals (boxes) are indicated.

rotations have also been observed in reservoirs in relation to massive fluid injection [*Martínez-Garzón et al.*, 2013, 2014b; *Schoenball et al.*, 2014]. These stress rotations have been shown to correlate with fluid injection rates in accordance with pore pressure changes (Figure 1) and reduced in situ temperatures by the cold fluid [*Jeanne et al.*, 2015; *Yoon et al.*, 2015]. In addition to these local perturbations, stress rotations depend mainly on the initial background stress [*Sonder*, 1990; *Zoback*, 1992]. Since the local perturbations in terms of the injection rate are known and an approximate knowledge of the reservoir rock properties is usually available, the initial differential stress as the remaining unknown can be estimated.

Herein, we demonstrate the feasibility of such initial differential stress estimation based on stress rotations. For this we use a generic, fully coupled 3-D thermo-hydro-mechanical (THM) model that simulates the pore pressure and thermal effects of cold fluid injection into a hot reservoir. In a systematic sensitivity study, (1) we assess the reservoir properties and treatment that are needed to cause a stress rotation and quantify the resulting angle of stress rotation. (2) We then discuss the key parameters and their influence on the occurrence of stress rotations and (3) derive from our findings an approach to estimate the initial differential stress of a reservoir with known properties from observed injection-induced stress rotations.

2. Stress Rotations

The in situ stress state is described by the symmetric second-order stress tensor with six independent components [*Zoback*, 2010; *Jaeger et al.*, 2007] or using the principal axis system with the three orientations and three magnitudes of the principal stresses $S1$, $S2$, and $S3$ [*Zang and Stephansson*, 2010; *Zoback*, 2010]. Isotropic changes in the stress state do not affect the orientation of these principal stress axes, but by changes in the differential stress $S1 - S3$ the orientation of the principal stress axes are potentially affected as well. This is, for example, the case for pore pressure changes due to reservoir depletion or injection. According to pore pressure stress coupling, the principal stresses are not equally reduced or increased by the pore pressure changes [*Rudnicki*, 1986; *Altmann et al.*, 2010, 2014; *Schoenball et al.*, 2010]. This means that the principal stress changes around an injection or production well are dependent on their position relative to the wellbore [*Altmann et al.*, 2014]. Hence, the differential stresses and therefore the orientation of the principal stress axes are altered.

The magnitude of anisotropic stress changes is dependent on several reservoir and material properties [*Rudnicki*, 1986] and controls the stress rotation. The angle of stress rotation itself is a manifestation of the physical response of a reservoir to fluid injection or depletion and thus depends on the magnitude of the initial differential stress, the material properties of the reservoir rock, and the reservoir treatment such as injection rate and fluid temperature. Thus, if stress rotations are observed and a sufficient amount of reservoir properties are known, the information can be used toward an improved geomechanical characterization of geological reservoirs.

An observation of injection-induced stress rotation is available from the NW part of The Geysers geothermal area, California [*Martínez-Garzón et al.*, 2013, 2014b]. A high-density seismic network of 32 permanent stations is deployed within the geothermal area [*Martínez-Garzón et al.*, 2013]. In the vicinity of the injection wells Prati-9 and Prati-29 within almost 5 years, 973 focal mechanisms from seismic events with moment magnitude M_w between 1.0 and 3.3 were computed [*Martínez-Garzón et al.*, 2014b]. A subsequent spatiotemporally binned stress inversion allowed the observation of rotations of the principal stress axes of up to 20° (Figure 1b) [*Martínez-Garzón et al.*, 2013, 2014b]. The time-dependent rotations of the principal stress axes correlate well with the variations in the monthly injection rates into the reservoir from both nearby wells (Figure 1a) [*Martínez-Garzón et al.*, 2013, 2014b]. The relationship between fluid injection and stress rotation has recently been observed in another part of The Geysers field [*Dreger et al.*, 2017] and was also confirmed by geomechanical-numerical modeling calibrated on The Geysers scenario [*Jeanne et al.*, 2015].

3. Generic Model

In order to identify the reservoir parameters controlling the stress rotations, we built a fully coupled generic 3-D thermo-hydrome-chanical (THM) model with isotropic and homogeneous rock properties. It has drained pore pressure and fixed temperature boundary conditions at the borders that are far away from the area of interest to prevent boundary effects and feedbacks (Figure 2c). The model simulates the injection of a cold fluid at a single point into the center of a fully saturated hot reservoir. The solution of the poroelastic equation [*Rudnicki*, 1986; *Altmann et al.*, 2010, 2014] implies that stress changes are independent of the initial stress state; the stress rotation, however, depends on the ratio of the initial differential stress and the stress changes. The effects of the coupled temperature and pore pressure changes on the stress field are simulated. The reservoir properties, treatment, and the initial differential stress can be easily altered in order to compare their influence on the angle of stress rotation. The properties of the reference model are presented in Table 1. They are chosen in a way to be comparable to values reported for The Geysers reservoir [e.g., *Rutqvist and Oldenburg*, 2008; *Rutqvist et al.*, 2013; *Jeanne et al.*, 2015] where injection-induced stress rotations have been observed. The parameters in italics in Table 1 are individually investigated in the sensitivity study with respect to the reference model. Several scenarios in which only a single parameter is altered from the reference value are computed in order to estimate the significance of the influence of the individual parameters on the stress rotation. The scenarios are chosen to represent a reasonable range of maximum and minimum values observed in reservoirs.

Due to the observation of stress rotations by the stress inversion of spatially binned focal mechanisms [*Martínez-Garzón et al.*, 2013], each rotation is actually an integral value valid for that particular rock volume. Hence, the volume enclosed by the seismicity in each stress inversion needs to be accounted for in the model as to guarantee comparison with the observations. Thus, the stress rotations in the model is regarded concerning the angle of rotation within an affected rock volume. The necessity to regard the reservoir volume

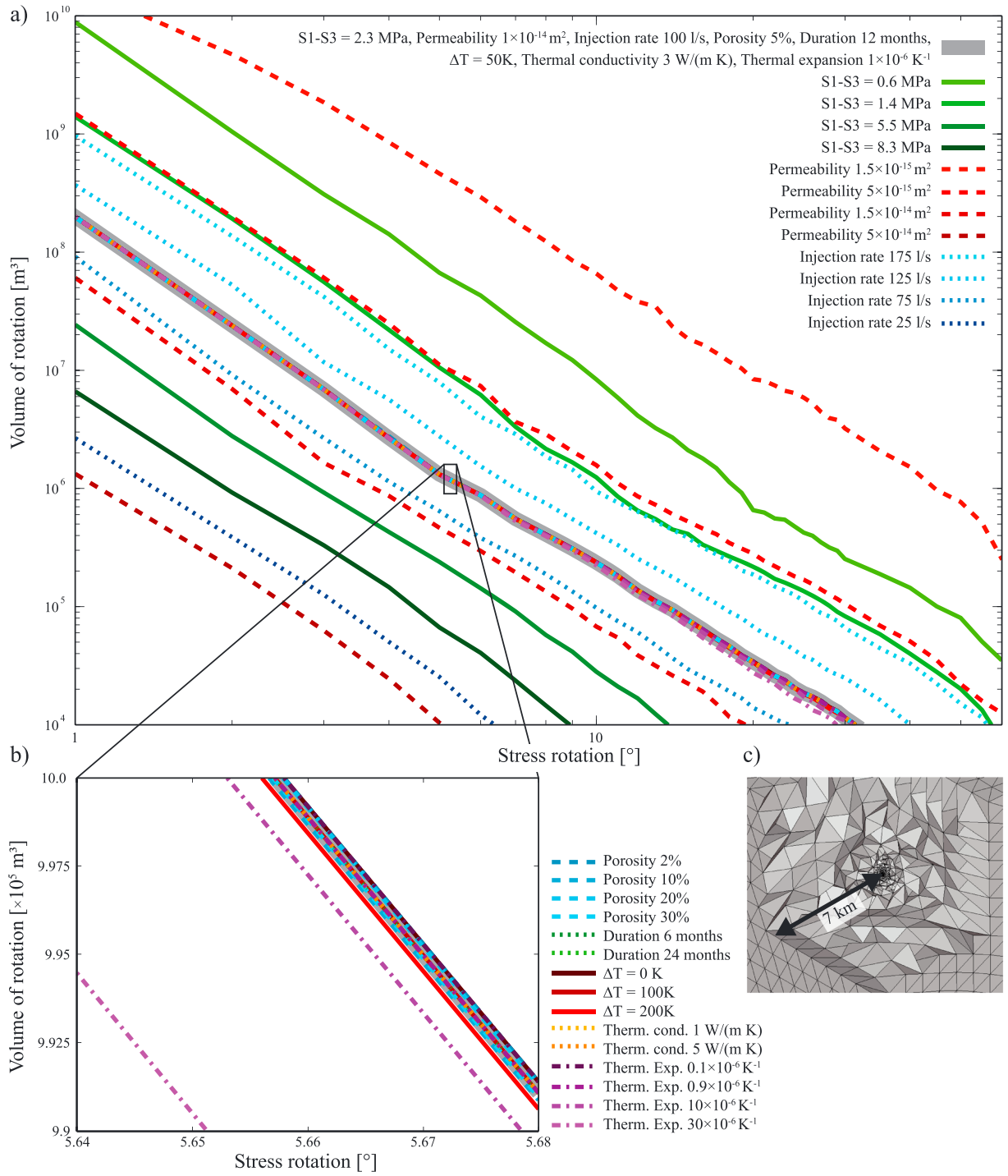

Figure 2. (a and b) Influence of several parameters on the rotation angle of the principal stress axes displayed in logarithmic scale. On the *x* axis is the stress rotation angle; on the *y* axis is the volume in m^3 affected by at least the stress rotation specified on the *x* axis. In relation to a reference scenario (grey solid) variable angles of stress rotations are indicated. They result from variations in the initial differential stress (green solid), permeability (red dashed), and injection rate (blue dotted) (Figure 2a). The insignificant influence of the porosity (blue dashed), duration of injection (green dotted), temperature difference (red solid) and thermal conductivity (orange dotted) on the stress rotation angle is displayed in a close-up together with the slightly more prominent influence of the thermal expansion of the rock (violet dash dotted) (Figure 2b). (c) A cut-view of the generic 3-D model indicates the refined discretization toward the injection point in the center of the model. The modeled injection point has a minimum distance of 7 km from the model boundaries.

Table 1. Reservoir Parameters in the Reference Model[a]

Material	Property Value	Minimum	Maximum
Rock density	2750 kg/m^3		
Young's module rock	26 GPa		
Poisson ratio rock	0.35		
Porosity rock[b]	5%	2%	30%
Permeability rock[b,c,d]	1×10^{-14} m^2	1×10^{-15} m^2	5×10^{-14} m^2
Bulk modulus solid grains[e]	50 GPa		
Drained bulk modulus[e]	26 GPa		
Thermal conductivity rock[f,g]	3 W/(m K)	1 W/(m K)	5 W/(m K)
Specific heat rock	800 J/(kg K)		
Latent heat	100 kJ/kg		
Thermal expansion[g]	1×10^{-6} K^{-1}	0.1×10^{-6} K^{-1}	30×10^{-6} K^{-1}
Density pore fluid[h]	1000 kg/m^3		
Latent Heat pore fluid[h]	350 kJ/kg		
Conductivity pore fluid[h]	0.6 W/(m K)		
Specific heat pore fluid[h]	4200 J/(kg K)		
Expansion[h]	Temperature dependent		
ΔT	50 K	0 K	200 K
Injection rate[i]	100 L/s	25 L/s	175 L/s
Injection duration	12 months	6 months	24 months
Differential stress	2.3 MPa	0.6 MPa	8.3 MPa

[a]The parameters in italics are regarded in the sensitivity analysis, and reasonable maximum and minimum values observed in reservoirs are provided. If no reference is provided, standard values are assumed.
[b]*Moeck* [2014].
[c]*Bear* [1972].
[d]*Martínez-Garzón et al.* [2014b].
[e]*Altmann et al.* [2010].
[f]*Robertson* [1988].
[g]*Rutqvist et al.* [2013].
[h]*IAPWS* [1997].
[i]*Zang et al.* [2014].

in which the stress rotation is estimated requires the 3-D analysis of the THM model. We use the finite element method with fully coupled partial differential equations for the thermoporoelastic processes. A finer resolution is achieved close to the injection point and a coarse resolution at the boundaries. The fluid injection is assumed to be constant during the entire injection time interval. The finite element solver Abaqus is applied to solve the resulting coupled partial differential equations which characterize the stress due to temperature and pore pressure changes. The equations result in the stress tensor, temperature, and pore pressure at each integration point in the entire model volume with no phase changes assumed.

4. Results

To derive the initial differential stress from stress rotations as a physical response of the reservoir to fluid injection, a sensitivity analysis is performed by investigating the key properties controlling the stress rotation. Then, a reservoir characterization approach is presented.

4.1. Sensitivity Analysis

For the sensitivity analysis the reservoir parameters porosity, permeability, thermal conductivity, thermal expansion, and the initial stress state and as the reservoir treatment parameters temperature difference between rock formation and injected fluid, injection rate, and injection duration were tested across physically reasonable ranges in reservoir environments (see Table 1). The analysis of the results is conducted in a volume-based approach rather than at discrete points in the reservoir. This is in order to be comparable to the observation of stress rotations by a spatiotemporally binned stress inversion of focal mechanism

solutions [*Martínez-Garzón et al.*, 2013]. Such observations are also within a confined volume in contrast to a single observation point.

Figure 2a shows that the results for the three significant parameters initial differential stress, permeability, and injection rate are a function of stress rotation within a given volume. An increase in initial differential stress is associated with a decrease in the volume affected by stress rotation. In the reference setting, a rotation of at least 15–20° in a volume of 10^6 m^3 requires a reduction of the initial differential stress to $S1-S3$ = 1.4 MPa. As for the rotation angle this refers to the minimum rotation that can be reliably observed from inversion of focal mechanisms given the fact that the inverted data (focal mechanisms) themselves include an error of typically not less than 10° [*Bohnhoff et al.*, 2004]. Moreover, a low permeability of the rock is beneficial for stress rotations to occur. A decrease in permeability from 1×10^{-14} m^2 to 5×10^{-15} m^2 has a similar effect as the reduction of initial differential stress by about $\Delta(S1\text{-}S3) = 1$ MPa. Furthermore, the injection rate is correlated with the stress rotation. Exemplified this means that an increase of the injection rate from 100 L/s to 200 L/s has about the same effect as a decrease in permeability from 1×10^{-14} m^2 to 5×10^{-15} m^2 or a reduction of the initial differential stress by $\Delta(S1-S3) = 1$ MPa.

Additionally, Figure 2b displays the parameters which prove to have no significant influence on the stress rotation. Changes in the porosity, the temperature difference between reservoir rock and injected fluid, the thermal conductivity of the rock, and the duration of constant injection prove to be entirely insignificant in a long-term scenario of ≥6 months. However, minor changes in the volume affected by stress rotation can be observed for changes in the thermal expansion of the rock. Still, rotations induced solely by thermal effects are not large enough to be considered relevant.

4.2. Effective Range of Key Parameters

The individual circumstances which favor or prevent the occurrence of a stress rotation are governed by the three key parameters permeability, initial differential stress, and injection rate. In order to investigate the numerical range in which these parameters allow a stress rotation, they are individually tested with realistic values. According to *Bear* [1972], the permeability in (oil) reservoir rocks is between 10^{-11} m^2 and 10^{-15} m^2. Differential stresses between $(S1-S3) = 0$ MPa and 40 MPa are likely to occur in reservoir settings [*Zang et al.*, 2012; *Brudy et al.*, 1997]. Typical injection rates during stimulation of (enhanced) geothermal reservoirs vary between 0.5 L/s and 175 L/s [*Zang et al.*, 2014]. The limit above which stress rotation is considered relevant is set to 5° in a volume of $25 \times 25 \times 25$ m^3 (=15,625 m^3).

It is revealed that in the range of realistic values, the permeability is the main and decisive factor which regulates the occurrence of stress rotation. In a semipermeable setting (10^{-12} m^2 according to *Bear* [1972]) a very high injection rate of 175 L/s and a very low differential stress ($S1-S3 = 0.6$ MPa) are required in order to generate a stress rotation above the limit. On the other hand, in an impermeable setting (10^{-15} m^2 according to *Bear* [1972]) with a medium differential stress (8.3 MPa) an injection rate of 7.5 L/s is sufficient to create stress rotations larger than the limit. If the initial differential stress is reduced to $S1-S3 = 0.6$ MPa, the same angle of rotation in the same volume is generated by 10% of the injection rate (0.75 L/s). This depicts the small extent of stress rotation control by the magnitude of initial differential stress in comparison to the permeability. In addition to an already low permeability, a small initial differential stress further increases the angle of stress rotation. However, even an unrealistically high value of $S1-S3 = 50$ MPa allows stress rotations above the limit as long as the permeability is low (10^{-15} m^2) and the injection rate high (175 L/s). The injection rate significantly controls the angle of the rotation. Yet it is not a decisive factor for the occurrence of stress rotations since unrealistically high injection rates ($\gg$200 L/s) are required to generate a rotation above the limit in a high permeability ($\geq 10^{-10}$ m^2) setting with a low differential stress ($S1-S3 = 0.6$ MPa). Even a further increase in the injection rate cannot counterbalance an additional increase in permeability and no stress rotations will occur.

4.3. Reservoir Characterization

The estimation of the differential stress is based on observations of the mean stress rotations by the stress inversion of spatially binned focal mechanisms and several modeled scenarios of stress rotation. The modeled scenarios are identical in their geometry and the reservoir properties and treatment with the exception of the initial differential stress which is altered in each scenario. Every modeled scenario simulates the stress rotation due to fluid injection into the reservoir. The simulated mean stress rotation is estimated in a volume that is equivalent to the volume used for the spatial binning of focal mechanisms in the stress inversion. The resulting

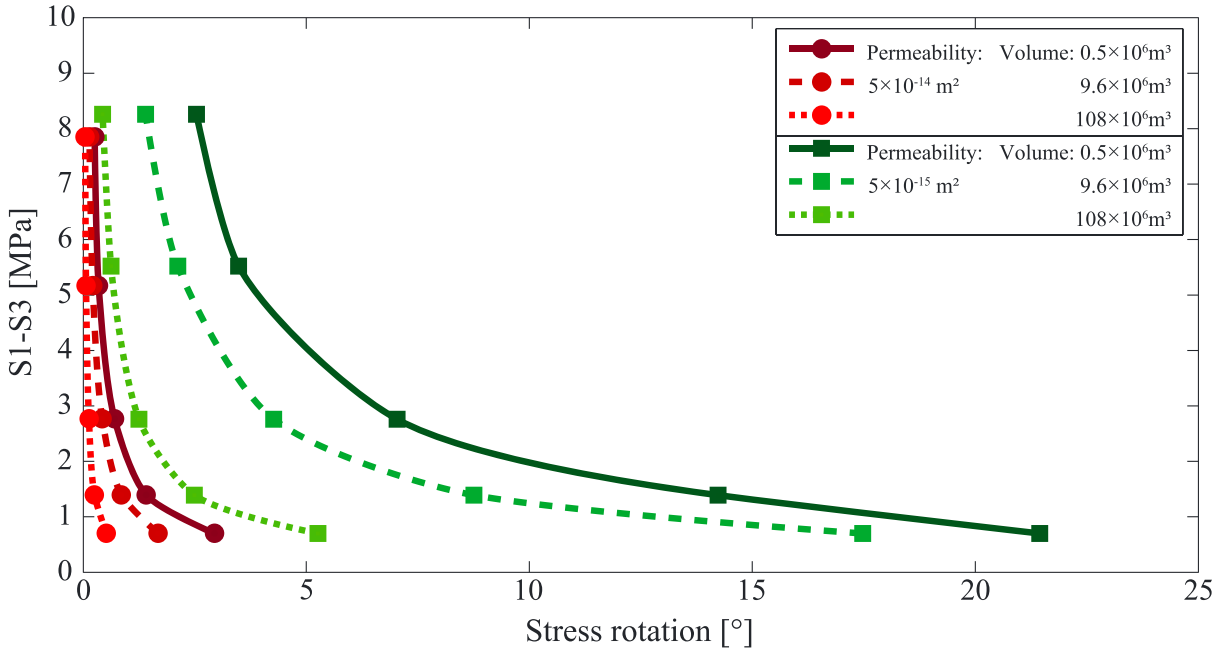

Figure 3. The initial differential stress as a function of stress rotation, permeability, reservoir characteristics, and volume of observed stress rotation. On the *x* axis is the stress rotation, on the *y* axis the initial differential stress. Two different permeabilities are assumed (5×10^{-14} m^2 (red) and 5×10^{-15} m^2 (green)), while all other reservoir characteristics remain the same. The stress rotation is evaluated within three different volumes around the injection point and averaged at 200 random locations. For each setting five model scenarios at different initial differential stresses are computed. This results in the displayed points that are used to interpolate reservoir specific curves. The curves depend on the initial differential stress, the permeability, and the regarded volume of interest.

scenario and reservoir specific relationships between the initial differential stress and the stress rotation are displayed in Figure 3.

In Figure 3 each of the dots and squares represents such a relationship between stress rotation and initial differential stress. Thus, each reservoir specific curve links the observed stress rotation with an initial differential stress state. As an example, two different reservoir permeabilities were assumed in Figure 3 (5×10^{-14} m^2, red and 5×10^{-15} m^2, green). The significant difference in modeled stress rotation between the two different permeabilities is in line with the previously indicated sensitivity analysis (see Figure 2). The higher permeability results in clearly smaller stress rotations for the same differential stresses compared to the permeability which is 1 order of magnitude lower (Figure 3). This is especially significant for low differential stresses and high stress rotations. Furthermore, for each permeability scenario the mean stress rotation was obtained in three different volumes (0.5×10^6 m^3, 9.6×10^6 m^3, and 108×10^6 m^3). This shows the dependency of the stress rotation on the distance to the injection point and the regarded volume respectively which is according to the findings presented in Figure 2. Due to the pore pressure diffusion an increase in volume for the estimation of the mean stress rotation results in a decrease of the mean rotation angle (Figure 3).

5. Discussion

In this work we investigate the controlling factors for injection-induced stress rotations. In order to identify the significant parameters, a sensitivity study provides the influence of reservoir properties and treatment on the stress rotation. It indicates that the parameters with the largest influence on the stress rotation are the known injection rate, the often estimated permeability of the reservoir, and the unknown initial differential stress. Other inherent reservoir properties such as porosity and thermal conductivity or reservoir treatment such as injection duration do not contribute in a significant extent to the development of stress rotation in a long-term scenario.

Among the three key parameters the permeability is identified to be the most influential one which partly owes to its large variety of observed values in reservoirs [*Bear*, 1972]. Moreover, a high permeability is the only parameter which is able to prevent stress rotations at all because in this case the poroelastic stress changes are negligible. Significant stress rotations are not expected in reservoirs with permeability larger than

approximately 10^{-13} m^2 even though theoretically stress rotations may occur in such settings due to very high injection rates (>150 L/s) or very low differential stress (<2 MPa). Conversely, a low injection rate (<10 L/s) and a high differential stress (>10 MPa) can significantly limit stress rotations even in a low permeability reservoir ($< 10^{-14}$ m^2).

In this work, a THM model was used to simulate stress rotations in a homogeneous isotropic generic test scenario. The described model is ready to alter material properties to relevant values for a certain reservoir type and even include anisotropies. Furthermore, the reservoir engineering parameters can be adapted to represent cyclic injection [*Zang et al.*, 2013; *Zimmermann et al.*, 2010], production and injection from the same well [*Tischner et al.*, 2010], different injection durations, and different injection temperature. The stress rotation angle is quite robust to small changes in injection rate. However, significant fluctuations are expected to result in clearly observable effects (Figure 1a). The approach can be easily adapted to include an actual reservoir geometry. The significance of the influence of reservoir features such as sealing and conducting faults, anisotropies, and inhomogeneities are expected to depend mainly on their deviation from the rest of the reservoir. Small deviations can be neglected. Furthermore, a more realistic injection geometry (line source) and lateral and vertical extent of the reservoir is expected to result in a similar stress rotation angle. Injection and production layouts featuring several boreholes will affect the stress rotation angle in a way that is mainly influenced by the communication of the wells and their distance. Such adaptions of the reservoir model improve the precision of the differential stress estimation approach for a distinct reservoir setting.

The primary challenges remain the precise detection and localization of induced seismic events and the availability of information on the permeability. Still, in case of large uncertainties in both parameters conclusive results are provided. In Figure 3 the permeability is between 5×10^{-15} m^2 and 5×10^{-14} m^2. If stress rotations of more than 7° are observed, an initial differential stress of maximum 3 MPa can be concluded. Furthermore, the permeability is then most likely in the area of 5×10^{-15} m^2. This knowledge of the differential stress in most tectonic settings allows the derivation of additional information on the stress state such as $S_{H\max}$ if the minimum horizontal stress $S_{h\min}$ and the vertical stress S_v magnitudes are available.

As an application to the geothermal reservoir characterization [*Moeck*, 2014] our results imply that significant stress rotations are to be expected in reservoirs dominated by crystalline rock, micritic carbonate rock, and sediments with a permeability of $< 10^{-15}$ m^2 (porosity <15%). The individual angle of stress rotation and affected volume is dependent on the site-specific injection rate and differential stress. Furthermore, rotations are expected for reservoirs in dolomitic carbonate rocks and sediments with permeabilities $< 5 \times 10^{-14}$ m^2 (porosity between 15 and 25%). In those settings rotations can be very small or even prevented if the differential stress is large. In addition, a low injection rate can mitigate the angle of stress rotations. Almost no stress rotations are expected in fracture- or karst-dominated reservoirs or sedimentary reservoirs with a high permeability ($> 10^{-13}$ m^2, porosity >25%). In most of those scenarios even very high injection rates and very low differential stress will not lead to a significant stress rotation due to the high permeability. In summary, stress rotations are mainly to be expected in petrothermal enhanced geothermal systems and their occurrence is likely in hydrothermal reservoirs which require stimulation. This could be the reason that to date, they have only been observed at The Geysers geothermal field. Hydrothermal systems are not prone to stress rotations since their initial permeability is usually already high effectively preventing stress rotations.

6. Conclusion

We apply a generic 3-D thermo-hydro-mechanical model to demonstrate that injection-induced stress rotations in a reservoir can be used to estimate the initial differential stress within a particular rock volume given certain rock permeability and fluid injection rates since they are the physical response of the rock to the injection. The approach requires detailed information on the injection rate and the reservoir permeability which are the most influential parameters. Any further reservoir and engineering properties are secondary for a successful application. In addition, it is indicated that thermal effects have no significant influence on stress rotations. Furthermore, we find that for common differential stress and reservoir treatments stress rotations are only expected in settings with a permeability of less than approximately 10^{-12} m^2. The presented approach can also be used to first order assess the expected stress rotations within a reservoir prior to injection. In addition, the mitigation of stress rotations by limitation of the injection rate can be estimated. Further investigations are required in order to address the sensitivity of the stress rotation angle to reservoir geometry, faults, anisotropies, and injection scenarios.

Acknowledgments
The authors would like to thank two anonymous reviewers whose comments significantly improved the manuscript. Furthermore, we would like to thank Birgit Müller who read and commented on a initial version of the manuscript. The research leading to these results has received funding from the European Community's Seventh Framework Programme under grant agreement 608553 (Project IMAGE). All data for this paper are properly cited and referred to in the reference list or presented in figures.

References

Altmann, J., B. Müller, T. Müller, O. Heidbach, M. Tingay, and A. Weißhardt (2014), Pore pressure stress coupling in 3D and consequences for reservoir stress states and fault reactivation, *Geothermics*, *52*, 195–204, doi:10.1016/j.geothermics.2014.01.004.

Altmann, J. B., T. M. Müller, B. I. Müller, M. R. Tingay, and O. Heidbach (2010), Poroelastic contribution to the reservoir stress path, *Int. J. Rock Mech. Min. Sci.*, *47*(7), 1104–1113, doi:10.1016/j.ijrmms.2010.08.001.

Bear, J. (1972), *Dynamics of Fluids in Porous Media*, Dover, New York.

Bohnhoff, M., S. Baisch, and H.-P. Harjes (2004), Fault mechanisms of induced seismicity at the superdeep German Continental Deep Drilling Program (KTB) borehole and their relation to fault structure and stress field, *J. Geophys. Res.*, *109*, B02309, doi:10.1029/2003JB002528.

Bohnhoff, M., H. Grosser, and G. Dresen (2006), Strain partitioning and stress rotation at the North Anatolian fault zone from aftershock focal mechanisms of the 1999 Izmit M_w = 7.4 earthquake, *Geophys. J. Int.*, *166*(1), 373–385, doi:10.1111/j.1365-246X.2006.03027.x.

Brown, E. E., and E. Hoek (1978), Trends in relationships between measured in-situ stresses and depth, *Int. J. Rock Mech. Min. Sci. Geomech. Abstr.*, *15*(4), 211–215, doi:10.1016/0148-9062(78)91227-5.

Brudy, M., M. D. Zoback, K. Fuchs, F. Rummel, and J. Baumgärtner (1997), Estimation of the complete stress tensor to 8 km depth in the KTB scientific drill holes: Implications for crustal strength, *J. Geophys. Res.*, *102*(B8), 18,453–18,475, doi:10.1029/96JB02942.

Cornet, F., J. Helm, H. Poitrenaud, and A. Etchecopar (1997), Seismic and aseismic slips induced by large-scale fluid injections, in *Seismicity Associated with Mines, Reservoirs and Fluid Injections*, edited by S. Talebi, pp. 563–583, Springer, Basel, Switzerland., doi:10.1007/978-3-0348-8814-1_12.

Dorbath, L., N. Cuenot, A. Genter, and M. Frogneux (2009), Seismic response of the fractured and faulted granite of Soultz-sous-Forêts (France) to 5 km deep massive water injections, *Geophys. J. Int.*, *177*(2), 653–675, doi:10.1111/j.1365-246X.2009.04030.x.

Dreger, D. S., O. S. Boyd, and R. Gritto (2017), Automatic moment tensor analyses, in-situ stress estimation and temporal stress changes at the Geysers EGS demonstration project, paper presented at 42nd Workshop on Geothermal Reservoir Engineering, Stanford Univ., Stanford, Calif., 13–15 Feb.

Fuchs, K., and B. Müller (2001), World stress map of the Earth: A key to tectonic processes and technological applications, *Naturwissenschaften*, *88*(9), 357–371, doi:10.1007/s001140100253.

Gritto, R., and S. P. Jarpe (2014), Temporal variations of V_p/V_s-ratio at The Geysers geothermal field, USA, *Geothermics*, *52*, 112–119, doi:10.1016/j.geothermics.2014.01.012.

Hardebeck, J. L. (2012), Coseismic and postseismic stress rotations due to great subduction zone earthquakes, *Geophys. Res. Lett.*, *39*, L21313, doi:10.1029/2012GL053438.

Hardebeck, J. L., and E. Hauksson (2001), Crustal stress field in Southern California and its implications for fault mechanics, *J. Geophys. Res.*, *106*(B10), 21,859–21,882, doi:10.1029/2001JB000292.

Hardebeck, J. L., and A. J. Michael (2006), Damped regional-scale stress inversions: Methodology and examples for Southern California and the Coalinga aftershock sequence, *J. Geophys. Res.*, *111*, B11310, doi:10.1029/2005JB004144.

Harris, R. A. (1998), Introduction to special section: Stress triggers, stress shadows, and implications for seismic hazard, *J. Geophys. Res.*, *103*(B10), 24,347–24,358, doi:10.1029/98JB01576.

Heidbach, O., and Z. Ben-Avraham (2007), Stress evolution and seismic hazard of the Dead Sea Fault System, *Earth Planet. Sci. Lett.*, *257*(1–2), 299–312, doi:10.1016/j.epsl.2007.02.042.

Heidbach, O., M. Tingay, A. Barth, J. Reinecker, D. Kurfeß, and B. Müller (2010), Global crustal stress pattern based on the World Stress Map database release 2008, *Tectonophysics*, *482*(1–4), 3–15, doi:10.1016/j.tecto.2009.07.023.

Heidbach, O., M. Rajabi, K. Reiter, M. Ziegler, and WSM Team (2016), World stress map database release 2016, doi:10.5880/WSM.2016.001.

IAPWS (1997), Revised release on the IAPWS industrial formulation 1997 for the thermodynamic properties of water and steam. [Available at http://www.iapws.org/.]

Ickrath, M., M. Bohnhoff, G. Dresen, P. Martínez-Garzón, F. Bulut, G. Kwiatek, and O. Germer (2015), Detailed analysis of spatiotemporal variations of the stress field orientation along the Izmit-Düzce rupture in NW Turkey from inversion of first-motion polarity data, *Geophys. J. Int.*, *202*(3), 2120–2132, doi:10.1093/gji/ggv273.

Jaeger, J., N. Cook, and R. Zimmerman (2007), *Fundamentals of Rock Mechanics*, 4th ed., 488 pp., Blackwell, Malden, Oxford, Carlton.

Jeanne, P., J. Rutqvist, P. F. Dobson, J. Garcia, M. Walters, C. Hartline, and A. Borgia (2015), Geomechanical simulation of the stress tensor rotation caused by injection of cold water in a deep geothermal reservoir, *J. Geophys. Res. Solid Earth*, *120*, 8422–8438, doi:10.1002/2015JB012414.

Lund, B., and M. Zoback (1999), Orientation and magnitude of in situ stress to 6.5 km depth in the Baltic Shield, *Int. J. Rock Mech. Min. Sci.*, *36*(2), 169–190, doi:10.1016/S0148-9062(98)00183-1.

Martínez-Garzón, P., M. Bohnhoff, G. Kwiatek, and G. Dresen (2013), Stress tensor changes related to fluid injection at The Geysers geothermal field, California, *Geophys. Res. Lett.*, *40*, 2596–2601, doi:10.1002/grl.50438.

Martínez-Garzón, P., G. Kwiatek, M. Ickrath, and M. Bohnhoff (2014a), MSATSI: A MATLAB package for stress inversion combining solid classic methodology, a new simplified user-handling, and a visualization tool, *Seismol. Res. Lett.*, *85*(4), 896–904, doi:10.1785/0220130189.

Martínez-Garzón, P., G. Kwiatek, H. Sone, M. Bohnhoff, G. Dresen, and C. Hartline (2014b), Spatiotemporal changes, faulting regimes, and source parameters of induced seismicity: A case study from The Geysers geothermal field, *J. Geophys. Res. Solid Earth*, *119*, 8378–8396, doi:10.1002/2014JB011385.

Martínez-Garzón, P., Y. Ben-Zion, N. Abolfathian, G. Kwiatek, and M. Bohnhoff (2016), A refined methodology for stress inversions of earthquake focal mechanisms, *J. Geophys. Res. Solid Earth*, *121*, 8666–8687, doi:10.1002/2016JB013493.

Moeck, I. S. (2014), Catalog of geothermal play types based on geologic controls, *Renewable Sustainable Energy Rev.*, *37*, 867–882, doi:10.1016/j.rser.2014.05.032.

Robertson, E. C., (1988), Thermal properties of rocks, *U.S. Geol. Surv. Open File Rep., 88-441*, Reston, Va.

Rudnicki, J. (1986), Fluid mass sources and point forces in linear elastic diffusive solids, *Mech. Mater.*, *5*(1986), 383–393, doi:10.1016/0167-6636(86)90042-6.

Rutqvist, J., and C. M. Oldenburg (2008), *Analysis of Injection-Induced Micro-earthquakes in a Geothermal Steam Reservoir, The Geysers Geothermal Field, California*, Lawrence Berkeley Natl. Lab., Berkeley, Calif.

Rutqvist, J., P. F. Dobson, J. Garcia, C. Hartline, P. Jeanne, C. M. Oldenburg, D. W. Vasco, and M. Walters (2013), The Northwest Geysers EGS demonstration project, California: Pre-stimulation modeling and interpretation of the stimulation, *Math. Geosci.*, *47*(1), 3–29, doi:10.1007/s11004-013-9493-y.

Schoenball, M., T. M. Müller, B. I. R. Müller, and O. Heidbach (2010), Fluid-induced microseismicity in pre-stressed rock masses, *Geophys. J. Int.*, *180*(2), 813–819, doi:10.1111/j.1365-246X.2009.04443.x.

Schoenball, M., L. Dorbath, E. Gaucher, J. F. Wellmann, and T. Kohl (2014), Change of stress regime during geothermal reservoir stimulation, *Geophys. Res. Lett.*, *41*, 1163–1170, doi:10.1002/2013GL058514.

Sonder, L. (1990), Effects of density contrasts on the orientation of stresses in the lithosphere: Relation to principal stress directions in the Transverse Ranges, California, *Tectonics*, *9*(4), 761–771.
Tischner, T., H. Evers, H. Hauswirth, R. Jatho, M. Kosinowski, and H. Sulzbacher (2010), New concepts for extracting geothermal energy from one well: The GeneSys-project, paper presented at World Geothermal Congress 2010, pp. 1–5, Bali, 25–30 Apr.
Yoon, J. S., G. Zimmermann, and A. Zang (2015), Numerical investigation on stress shadowing in fluid injection-induced fracture propagation in naturally fractured geothermal reservoirs, *Rock Mech. Rock Eng.*, *48*, 1439–1454, doi:10.1007/s00603-014-0695-5.
Zang, A., and O. Stephansson (2010), *Stress Field of the Earth's Crust*, Springer, Netherlands, doi:10.1007/978-1-4020-8444-7.
Zang, A., O. Stephansson, O. Heidbach, and S. Janouschkowetz (2012), World stress map database as a resource for rock mechanics and rock engineering, *Geotech. Geol. Eng.*, *30*(3), 625–646, doi:10.1007/s10706-012-9505-6.
Zang, A., J. S. Yoon, O. Stephansson, and O. Heidbach (2013), Fatigue hydraulic fracturing by cyclic reservoir treatment enhances permeability and reduces induced seismicity, *Geophys. J. Int.*, *195*(2), 1282–1287, doi:10.1093/gji/ggt301.
Zang, A., V. Oye, P. Jousset, N. Deichmann, R. Gritto, A. McGarr, E. Majer, and D. Bruhn (2014), Analysis of induced seismicity in geothermal reservoirs—An overview, *Geothermics*, *52*, 6–21, doi:10.1016/j.geothermics.2014.06.005.
Zimmermann, G., I. Moeck, and G. Blöcher (2010), Cyclic waterfrac stimulation to develop an enhanced geothermal system (EGS)—Conceptual design and experimental results, *Geothermics*, *39*(1), 59–69, doi:10.1016/j.geothermics.2009.10.003.
Zoback, M. (2010), *Reservoir Geomechanics*, 461 pp., Cambridge Univ. Press, Cambridge, U. K.
Zoback, M. L. (1992), First- and second-order patterns of stress in the lithosphere: The World Stress Map Project, *J. Geophys. Res.*, *97*(B8), 11,703–11,728, doi:10.1029/92JB00132.